An evaluation of Re, as an alternative to Pt, for the 1 bar loop technique: An experimental study at 1400 °C

ALEXANDER BORISOV* AND JOHN H. JONES

SN2, NASA/Johnson Space Center, Houston, Texas 77058, U.S.A.

ABSTRACT

Previous investigators have shown that, at high pressure, Re is a good capsule material and that Fe loss to Re under these conditions is minimal (e.g., Herzberg and Zhang 1997). We present here the first systematic low-pressure study of Re loop stability and of Fe loss from silicate melts to Re loops as a function of f_{O_2}. Experiments were performed at 1400 °C and one bar pressure over a range of f_{O_2}. For f_{O_2} values as low as QFM-2, Fe loss was found to be negligibly small, even for a charge/loop ratio of only about 2. According to our calculations, for the same conditions, Fe loss to a Pt loop could reach 70% of the initial FeO content. We have also estimated the diffusion coefficient of Fe in Re and found it to be very small ($\approx 10^{-12}$ cm^2/s), which is an additional factor in preventing Fe loss.

At values of f_{O_2} near QFM, Re metal reacts to form volatile Re oxides. But at f_{O_2} below QFM-1.7, Re loops were found to be stable for any reasonable experimental run duration at 1400 °C. At lower temperatures Re may be stable to even higher values of f_{O_2}. These conditions are similar to or slightly more reducing than the accepted redox states for the mantles of the Earth and Mars. Consequently, for many experiments, Re may be a more convenient loop material than Pt.

INTRODUCTION

The container problem in experimental igneous petrology is an old and well-established one (e.g., Basaltic Volcanism Study Project 1981, p. 517–519). Platinum is a soft, flexible, and relatively cheap noble metal with a high melting temperature (1769 °C), and it has been used widely as loop material in low-pressure experiments. Unfortunately, the significant affinity of Fe for Pt metal can result in large Fe losses from FeO-containing systems, especially at low values of f_{O_2}. Such loss can seriously change not only phase relations and compositions in long-duration experiments, but also the texture, mineralogy, and chemical zoning of products in short, dynamic-crystallization experiments (Lofgren et al. 1979; Weinbruch et al. 1998). Presaturation of Pt metal with Fe is a time-consuming technique and needs an exact knowledge of the Fe-Pt alloy composition for every experimental condition (e.g., Grove 1981; McKay et al. 1994). For this reason commercially available noble metal alloys (Ag-Pd, Au-Pd, Au-Pt) also have been widely used in experimental petrology for the reduction of Fe loss, although without great success (Stern and Wyllie 1975; Biggar 1977). The calculated affinities of Fe for different noble metals (Borisov and Palme, unpublished manuscript) showed that, with the exception of Au, whose melting temperature (1064 °C) is too low for many experiments, only Ru and Ir are likely to be useful alternatives to Pt. Unfortunately, the brittleness of Ir wires and the absence of commercially available Ru wire would make the use of these metals impracticable.

Rhenium is one of the less-common refractory metals and has the second highest melting temperature (3186 °C). At high pressure, Fe loss to Re is greatly reduced compared to Pt (e.g., Herzberg and Zhang 1997). Unfortunately, Re metal is not stable over as wide a range of redox conditions as Pt. At only modestly oxidizing conditions ($\approx$QFM), Re reacts with oxygen to form volatile Re oxides, destroying the loop and ruining the experiment.

Here we present the results of a systematic investigation of (1) metallic Re volatility under controlled oxygen fugacities; (2) Fe loss from FeO-containing melts suspended from Re loops; and (3) the diffusion rate of Fe in metallic Re. Thus, this study delimits practical guidelines for the use of Re as a container material in experimental petrology and geochemistry.

RHENIUM VOLATILITY AS A FUNCTION OF OXYGEN FUGACITY

Experimental procedures

All experiments were conducted in a Deltech vertical-tube, 1 atm furnace, where the f_{O_2} was controlled by CO/CO$_2$ gas mixtures. A PtRh$_6$/PtRh$_{30}$ thermocouple in the working furnace and a ZrO$_2$ solid-electrolyte oxygen sensor in a remote furnace were employed for measuring temperature (± 2 °C) and f_{O_2} (± 0.1 log unit) during experimental runs. Experiments were performed at a constant temperature of 1400 °C over a range of f_{O_2} from $10^{-3.0}$ (pure CO$_2$) to $10^{-10.4}$ atm (4 log units below the QFM buffer). Total gas linear velocity through the furnace was 0.76 cm/min for most experiments and was adjusted with a gas flowmeter (Matheson, model 10220) with an accuracy of ± 0.07 cm/min.

One or two short pieces (2–6 mm long) of Re wire (99.97% purity, Alfa) with a nominal diameter of 0.25 mm (0.246 mm, according to our measurements) were placed in a small silica crucible and suspended in the hot zone of the furnace for a fixed period of time at fixed f_{O_2} (Table 1). The Re wires were

---

*E-mail: aborisov@ems.jsc.nasa.gov

weighted accurately (Sartorious, Supermicro) before and after the experiment. Additionally, the average diameter of the processed wires was measured with an accuracy of ±0.0025 mm.

Experimental results: Re loop stability at different f_{O_2}

Experimental results are given in Table 1. Relative Re losses per unit time are plotted vs. log f_{O_2} in Figure 1. As expected, there is a general trend of decreasing volatility with decreasing f_{O_2}. However, the relationship appears to be divided into three discrete regions. In region I (f_{O_2} <10$^{-8.0}$ atm), evaporation is very slow and depends weakly, if at all, on f_{O2}. The "half-life" of the Re loop (50% evaporation of Re wire) in region I was calculated to be on the order of weeks (see Fig. 1).

In region II (f_{O_2} between 10$^{-5.8}$ and 10$^{-8.0}$ atm), Re volatility increases dramatically with increasing f_{O_2} and the "half-life" at f_{O_2} >QFM does not exceed a few hours. Thus, experiments with Re loops at 1400 °C may only be conducted at f_{O_2} values well below 10^{-7} atm.
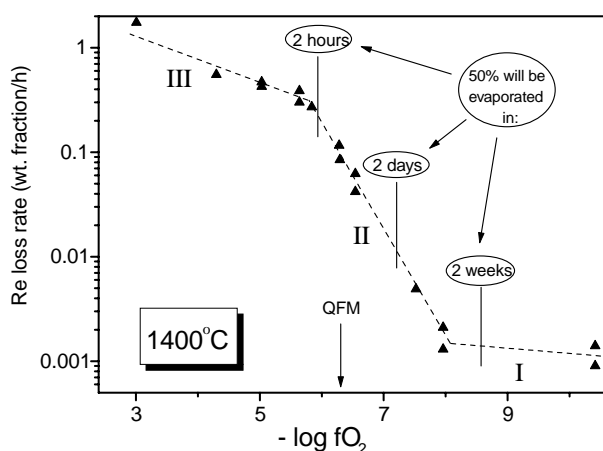

FIGURE 1. Relative weight loss of Re wire pieces vs. oxygen fugacity. Three different f_{O_2} ranges with different regimes of volatility are indicated by the Roman numerals.

In region III (f_{O_2} >10$^{-5.8}$ atm), volatile loss of metallic Re is extremely rapid. For example, in pure CO_2 the Re wire would be expected to evaporate completely within one hour (see Table 1).

It is obvious that the different slopes of Re loss vs. log f_{O_2} reflect different mechanisms of Re evaporation, and this is discussed in more detail in the Appendix. But what is important from a practical point of view is that at high temperature (1400 °C) and f_{O_2} values below 10^{-8} atm (QFM-1.7), a Re container will be quite stable during any reasonable experimental duration.

IRON LOSS FROM FeO-CONTAINING MELTS SUSPENDED FROM RE LOOPS

Experimental procedures

All experiments were conducted in the same furnace at a constant temperature of 1400 °C over a range of f_{O_2} from 10$^{-7.7}$ (IW+2) to 10$^{-10.5}$ atm (IW–1). All experiments had nearly the same run duration of 45 ± 2 hours (Table 2).

A commercially available Re ribbon ("Goodfellow," 99.99% purity, 0.76 mm wide, and 0.05 mm thick) was used as a loop material. Strips were cut from this ribbon and loops with an average diameter of 2.5 mm were formed at the end of the longer strip, with the final product resembling a "δ". This looped strip was then attached to a hanging rod using Pt wire, with the Pt-Re contact at the top of the "δ".

Synthetic melts in the pseudobinary system "anorthite-diopside eutectic+FeO" with initial total FeO contents of 8.2 wt% (DAF10), 16.6 wt% (DAF20), and 35.0 wt% (DAF40) were used in the experiments. Anorthite-diopside eutectic glass was spiked with FeO in appropriate proportions and homogenized in an agate mortar. The DAF10 mixture is a good analog for terrestrial basalts, DAF20 approximates the FeO content of lunar, martian, and asteroidal ("planetary") basalts, and the DAF40 composition is an Fe-slag type melt that was employed to make small degrees of Fe loss more obvious. Silicate powders mixed with a glue were inserted into the loops, which were then suspended from a ceramic disk and transferred into the furnace.

The average melt/loop mass ratio was about 2 and was nearly constant for all experimental charges. Samples were quenched

TABLE 1. Metallic Re volatility: experimental conditions and results

No.	Sample	V gas, cm/sec	–log f_{O_2}	t,C	*hs	†Weight, mg I.W.	A.W.	‡D, mm	§Re loss, wt. frac./h
1	RE10	0.76	3.01	1400	0.38	3.41	1.15	0.150	1.743
2	RE9	0.76	4.30	1399	0.45	4.29	3.22	0.226	0.553
3	RE8	0.76	5.03	1399	0.43	5.46	4.36	0.229	0.468
4	RE8a	0.76	5.03	1399	0.43	3.57	2.92	0.229	0.425
5	RE6	0.76	5.64	1397	0.40	6.19	5.24	0.236	0.387
6	RE6a	0.76	5.64	1397	0.40	2.73	2.40	0.236	0.300
7	RE5	0.76	5.84	1397	0.57	4.59	3.88	0.234	0.271
8	RE2	0.76	6.28	1400	2.12	3.86	2.91	not md.	0.116
9	RE3	0.76	6.29	1398	1.92	5.51	4.62	0.239	0.085
10	RE11	0.76	6.54	1398	5.72	4.87	3.14	0.226	0.062
11	RE11a	0.76	6.54	1398	5.72	2.58	1.96	0.229	0.042
12	RE4	0.76	7.52	1399	14.17	5.23	4.87	0.239	0.005
13	RE7	0.69	7.96	1400	24.48	6.37	6.05	0.244	0.002
14	RE7a	0.69	7.96	1400	24.48	3.84	3.72	0.244	0.001
15	RE16	0.73	10.41	1394	63.08	5.11	4.66	0.241	0.001
16	RE16a	0.73	10.41	1394	63.08	2.53	2.39	0.244	0.001

* Experimental duration, in hours.
† I.W. = initial weight, before experiment; A.W. = weight after experiment.
‡ Diameter after experiment.
§ Re loss = (ini. weight - aft. weight)/h.

by quickly withdrawing the hanging rod from the hot zone to the top of the furnace.

Quenched samples were mounted in epoxy and polished. Glasses were analyzed for major elements with a Cameca Camebax electron microprobe. Natural pyroxene was used as a standard for all elements. Iron in Re loops was analyzed with a Cameca SX-100 electron microprobe. Operating conditions were 20 kV accelerating voltage and 20 nA beam current, with Fe metal as a standard for Fe. In addition, Fe diffusion profiles were measured in the loop at loop/glass contacts, using 1 μm steps and 60 s counting times on Fe$K\alpha$ X-rays.

Results and discussion: Fe loss from experimental melts

In most cases, glasses had the shape of cylinders with flat to slightly rounded surfaces, and the outer loop surface was clean of silicate. However, the outer surfaces of the loops in the most-reducing experiments with the highest FeO contents (DAF40 series below $10^{-9.6}$ atm) were covered with a thin layer of melt. Apparently, there is an increase in the tendency of the silicate to wet the metal as the Fe content of the Re metal increases (for a more detailed discussion, see below). The most-reducing loop (DAF40-4) was seriously deformed, implying that, at f_{O_2} values below $10^{-10.5}$ atm, the combination of Re loops and Fe-rich melt compositions should be used carefully.

All glasses are essentially homogeneous with respect to FeO, reflecting much faster diffusion in the silicate melt compared to the metal, where Fe analysis reveals highly zoned profiles that are attributable to diffusion of Fe into the Re. The average Fe contents of the experimental glasses are given in Table 2 and displayed graphically vs. log f_{O_2} in Figure 2.

There was practically no Fe loss from the silicates containing 8.2 wt% FeO (DAF10 series) down to QFM-2, and the Re loops of this series contained much less than 1 wt% Fe (see below for details). Even at IW-0.5, only ~14% FeO loss was observed. We compared these experimental results with calculations of Fe loss to Pt loops, assuming complete equilibrium and the same Pt/silicate ratio (thermodynamic data for the Fe-Pt binary are taken from Heald 1967). Based on these calculations (QFM-2 and 1400 °C), we anticipate that about 70% of the initial Fe would be lost in Pt from our "terrestrial basaltic" melts.

Iron loss from "planetary basalts" (DAF20 series) is a little higher than from "terrestrial basalts" (5% of initial FeO at QFM-

1.9 and ~12% at IW-0.5), but still considerably lower than would be expected for a Pt loop (>50% at QFM-2). Also, we will argue below that the DAF20 results at QFM-2 are probably atypical, although the reason for this is unclear.

Finally, Fe loss from our "Fe-rich slags" (DAF40 series) is only ~1% at QFM-2 (calculated loss to a Pt loop would be ~30% at the same conditions). Iron loss still stays reasonably low (15%) at IW buffer conditions, and only approaches 50% at IW-1.

The small amounts of Fe loss at QFM-2 for both the DAF10 and DAF40 series are the main reason we believe the higher loss experienced by the DAF20 experiment at the same f_{O_2} is not representative. This is best shown by Figure 3, which illustrates the functional relationship between the percentage of Fe lost and f_{O_2}. With the exception of the DAF20 series experiment at QFM-2, the data of all experiments form a very consistent trend. The regression line ($R^2 = 0.994$) is not for the entire data set but is fitted to the DAF40 series only, where small changes in Fe loss are quantified most easily. Clearly, the DAF40 regression is also consistent with the overall data set. Thus, the equation:

$$\log (\text{percent Fe loss}) = -0.75\ (\pm 0.03) \times \log f_{O_2} - 6.17\ (\pm 0.07, 1\sigma) \quad (1)$$

can be used for the rough estimation of the *upper* limit (remember our low melt/loop mass ratio) of Fe loss from experimental charges at 1400 °C. The consistency among the different compositional series gives us increased confidence in the results of our experiments.

As expected, Fe loss to the Re loops increases (FeO content in glasses decreases) with decreasing f_{O_2} (see Figs. 2 and 3). Two main factors are responsible for Fe loss in any metal container: the low f_{O_2} and the mass melt/loop ratio ($R_{m/l}$). The equilibrium silicate melt/Re metal distribution of Fe can be described by the reaction:

$$\text{Fe (Re)} + 0.5\ O_2 = \text{FeO (silicate melt)} \quad (2)$$

The equilibrium constants of reactions 2 are given by:

$$K_2 = a_{FeO}/[a_{Fe} \times (f_{O_2})^{0.5}] \quad (3)$$

so the equilibrium Fe ratio is:

$$C_{melt}^{FeO}/C_{Re}^{Fe} = A \times (f_{O_2})^{0.5} \quad (4)$$

TABLE 2. Iron loss in Re loops: experimental conditions and FeO content in quanched glasses

No.	Sample	−log f_{O_2}	T °C	*hs	FeO, wt%	(1σ)
1	DAF10-5	7.69	1399	47	8.10	(0.13)
2	DAF40-5	7.69	1399	47	34.86	(0.16)
3	DAF20-2	8.17	1398	43	15.75	(0.10)
4	DAF10-9	8.32	1398	45	8.16	(0.03)
5	DAF40-9	8.32	1398	45	34.63	(0.42)
6	DAF10-8	8.97	1400	47	7.95	(0.18)
7	DAF40-8	8.97	1400	47	33.30	(0.14)
8	DAF20-1	9.36	1398	46	15.46	(0.09)
9	DAF20-6	9.70	1398	46	15.05	(0.09)
10	DAF40-6	9.70	1398	46	29.87	(0.05)
11	DAF20-7	10.06	1395	48	14.54	(0.02)
12	DAF40-7	10.06	1395	48	27.03	(0.18)
13	DAF10-11	10.09	1398	45	7.05	(0.06)
14	DAF40-4	10.52	1399	47	17.47	(0.21)

Notes: The same last numbers in the sample coldes mean that the charges were melted in the same experimental run; s.d. = standard deviation.
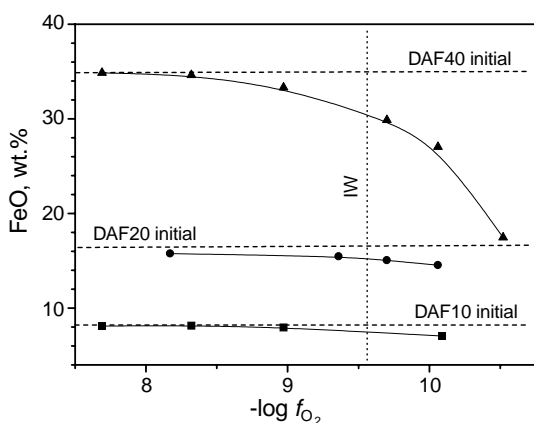* Duration of experiment in hours.

FIGURE 2. A plot of FeO vs. log f_{O_2} showing the Fe content of silicate glasses from three different series (DAF10, DAF20, and DAF40; initial FeO levels are shown with dashed lines) after experimental runs on Re loops at different oxygen fugacities (see text for details). All experiments were carried out at 1400 °C for approximately two days. FeO in the silicate decreases as Fe alloys with the Re loop.
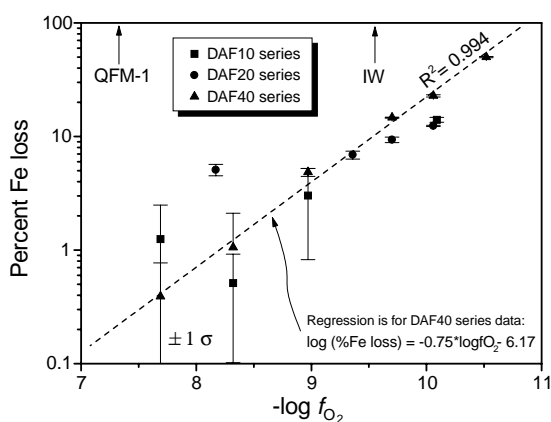

FIGURE 3. A plot of percent Fe loss vs. log f_{O_2}. All experiments seem to obey the same rate loss law, regardless of absolute FeO concentration.

where the constant A includes terms such as K_2, γ_{Fe} (Re), and γ_{FeO} (melt). Thus, the lower the f_{O_2}, the lower the equilibrium C_{melt}^{FeO}. The higher the value of $R_{m/l}$, the smaller the Fe loss for the same equilibrium $C_{melt}^{FeO}/C_{Re}^{Fe}$ ratio. We have already mentioned that in our experiments the average $R_{m/l}$ value was ~2, because the purpose of these experiments was not to prevent Fe loss, but to understand how serious it could be. Our experience in working with metal strip loops shows that $R_{m/l}$ can be easily increased to 10, which would result in even lower losses of Fe.

IRON DIFFUSION COEFFICIENTS IN METALLIC RHENIUM

In addition to the two equilibrium factors responsible for Fe loss (f_{O_2} and $R_{m/l}$), we should also mention a third kinetic one, the diffusion rate of Fe in Re. If, for example, there was a container material in which Fe diffusion was extremely slow, then Fe loss could be very small even for low f_{O_2} and $R_{m/l}$ values.

Analyzed profiles of Fe in Re showed that, in most cases, only the first 10 μm of the loop in contact with the silicate showed any Fe enrichment. And even in this case the amount of Fe was small, typically not exceeding 1 wt%. These Fe concentration profiles are typically irregular, perhaps because of the multi-crystalline nature of the Re metal. Therefore, it is possible that transport of Fe in Re is a complicated mix of faster intergranular (surface) diffusion and slower bulk diffusion.

Rhenium has an hexagonal crystal structure. Microscopic examination of a piece of the Re strip reveals the presence of many microcracks roughly perpendicular to the long dimension of the strip, which cross each other at angles of ~60° and 120°. The length of these cracks varies from 5 to 100 μm.

A few regular Fe profiles suitable for diffusion coefficient calculations were also found, and one of the best examples is shown in Figure 4. Our loop diameter was large enough and the Fe content of the silicate constant enough that, as a first approximation, we decided to use a diffusion model of a semi-infinite medium with initially zero Fe content and whose surface is maintained at a constant concentration C_0 (Crank 1975, Eq. 2.45):

$$C_{Re}^{Fe} = C_0 \times \text{erfc} \, [x/2(Dt)^{0.5}] \qquad (5)$$

where C_{Re}^{Fe} is the Fe content of Re along distance x from the silicate/metal boundary after experimental duration t, D is the diffusion coefficient, and erfc(z) is a complement to the error function erf(z), that is: erfc(z) = 1 − erf(z). We can rearrange Equation 5 as follows:

$$\text{inverf} \, (1 - C_{Re}^{Fe}/C_0) = x/2(Dt)^{0.5} \qquad (6)$$

If our simplifying assumptions are correct, the *inverse* error function of $(1 - C_{Re}^{Fe}/C_0)$ plotted vs. distance x should yield a straight line of slope $1/[2(Dt)^{0.5}]$. Accordingly, for known t, D can be calculated easily, as inverf(z) is a standard function in some commercially available software (e.g., Origin, Microcal Software, Inc). The value of C_0 is unknown, but can be estimated by trial and error by requiring that the trend pass through the origin.

The inset of Figure 4 plots inverf of $(1 - C_{Re}^{Fe}/C_0)$ as a function of distance for the first 8 μm of analyses shown in the main figure, because these are the only analyses that have sufficient Fe to constrain the model. We find that this simple model fits the Fe data very well and yields $C_0 = 0.30$ wt% and $D_{Re}^{Fe} = (5.3 \pm 0.2) \times 10^{-13}$ cm²/s. The true error in D_{Re}^{Fe} determination is probably somewhat higher than that indicated by our regression. If we assume ±0.5 μm as an accuracy for the location of the silicate/metal boundary, this becomes about 10% accuracy in our estimate of C_0, which will in turn result in a 3% error in the slope calculation and a 6% error in the determination of D_{Re}^{Fe}. Keeping in mind the simplicity of the model, this precision seems very acceptable. Other profiles of poorer quality gave D_{Re}^{Fe} in the same range: $4 - 10 \times 10^{-13}$ cm²/s. Thus, Fe diffusion in Re seems to be about three orders of magnitude slower than in Pt ($\approx 7 \times 10^{-10}$ cm²/s at 1400 °C, Berger and Schwarz 1978). Simplified calculations (for a plane bounded by one impermeable surface and one surface maintained at a constant Fe concentration) indicate that 10 hours at 1400 °C
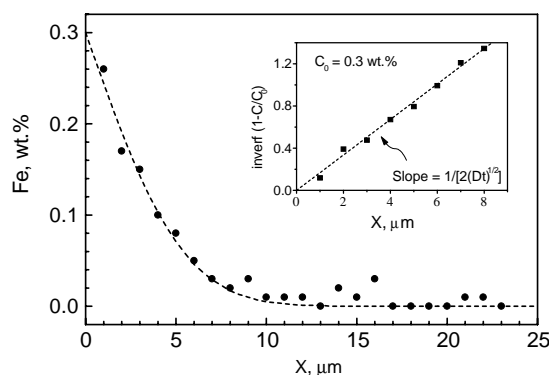
FIGURE 4. An example of a diffusive Fe profile through the Re loop of the DAF10-8 experimental charge. This inverse error function of this profile (inset) was used to calculate the diffusion coefficient of Fe in Re (see text for further explanation). At 1400 °C, the diffusivity of Fe as a tracer in Re metal is $\approx 5 \times 10^{-13}$ cm^2/s, which is much lower than the corresponding diffusivity in Pt at the same temperature.

would be sufficient to saturate and homogenize ($C_{min}/C_{max} > 0.9$) a Pt ribbon with a thickness (50 μm) similar to the Re in our experiments. This result is in contrast to our experiments, which showed practically no Fe in the Re loop at distances greater than 10 μm from the loop surface after 45 hours.

The foregoing discussion, however, is applicable only in cases where Fe concentrations in Re are low and approximate tracer diffusion. Under more reducing conditions, Fe concentrations may increase significantly and the situation can change dramatically. Self-diffusion of Fe in iron metal at 1400 °C, calculated from compilation of Askill (1970) is about $(6 \pm 1) \times 10^{-8}$ cm^2/s, which is about five orders of magnitude faster than tracer diffusion of Fe in Re. Thus, one could logically expect a large decrease for D_{Re}^{Fe} in Fe-rich Re-Fe alloys, compared to Fe-poor ones. Indeed, in our DAF20-7 experiment (IW-0.5), the first 20 mm of Re metal are both more enriched in Fe (1.5–2.5 wt%) and have profiles that are shallower, compared to more oxidizing experiments. However, the extreme example from our study is the DAF40-4 experiment, performed at IW-1, which is discussed in the Appendix.

CONCLUDING REMARKS

Our present results give clear estimates of the f_{O_2} range where Re loops could be used successfully. At 1400 °C experiments of several days are possible at QFM-2. At somewhat lower temperatures (1350–1250 °C), these same durations can be achieved at QFM-1 (J. Jones, unpublished data). These temperatures are quite hot, even by the standards of experimental igneous petrology, and it is possible that, at temperatures more typical of terrestrial basaltic liquidi (1250–1150 °C), even higher redox conditions are attainable. Consequently, we believe that, in many cases, Re may be an improvement over Pt as an experimental container.

Re is not much more expensive than Pt. The 2 m Re ribbon from "Goodfellow," which was used in these particular experiments, is now available for $371 (about 100 loops can be fashioned from this amount of Re). We were also quoted a price of ~$30/m for 0.1 mm thick Re wire by Rhenium Alloys, Inc.,

which is very similar to the cost of Pt wire of the same size. Taking into account the time and cost of electroplating Fe onto Pt wire (see Grove 1981 for details), it seems clear that in many cases Re may be a better choice than Pt.

REFERENCES CITED

Askill, J. (1970) Tracer Diffusion Data for Metals, Alloys, and Simple Oxides. IFI/ Plenum Data Corporation, New York.

Barin, I., Ed. (1995) Thermochemical data of pure substances. 3d ed., volumes I and II, Springer-Verlag, New York.

Basaltic Volcanism Study Project (1981) Basaltic Volcanism on the Terrestrial Planets, 1286 p. Pergamon Press, Inc., New York.

Battles, J.E., Gundersen, G.E., and Edwards, R.K. (1968) Mass spectrometric studies of the rhenium-oxygen system. Journal of Physical Chemistry, 72, 3963–3969.

Berger, D. and Schwarz, K. (1978) Zur Fremddiffusion in Platin. Neue Hütte, 23, 210–212.

Biggar, G. (1977) Some disadvantages of Pt$_{95}$Au$_5$ as a container for molten silicates. Mineralogical Magazine, 41, 555–556.

Cotton, F.A. and Wilkinson, G. (1966) Advanced Inorganic Chemistry: A Comprehensive Text, 2nd. ed., p. 1136. Interscience, New York.

Crank, J. (1975) The Mathematics of Diffusion. 2nd ed. Oxford University Press, Oxford, U.K.

Feynman, R.P., Leighton, R.B., and Sands, M. (1964) The Feynman Lectures on Physics, vol. II, p. 41–1. Addison-Wesley, Menlo Park, California.

Franklin, J.E. and Stickney, R.E. (1971) A simplified experimental method for determining the thermochemical properties of certain volatile species; application to ReO$_2$ and ReO$_3$. High Temperature Science, 3, 401–411.

Grove, T.L. (1981) Use of FePt alloys to eliminate the Fe loss problem in 1 atmosphere gas mixing experiments: Theoretical and practical considerations. Contributions to Mineralogy and Petrology, 78, 298–304.

Heald, E.F. (1967) Thermodynamics of Fe-platinum alloys. Transactions of Metallurgical Society AIME, 239, 1337–1340.

Herzberg, C. and Zhang, J. (1997) Melting experiments on komatiite analog compositions at 5 GPa. American Mineralogist, 82, 354–367.

Knacke, O., Kubashewski, O., and Hesselmann, K., Eds. (1991) Thermochemical data of pure substances. 2d Ed., volumes I and II, Springer-Verlag, New York.

Lofgren, G.E., Grove, T.L., Brown, R.W., and Smith, D.P. (1979) Comparison of dynamic crystallization techniques on Apollo 15 quartz normative basalts. Proceedings of Lunar and Planetary Science Conference 10th, 423–438.

McKay, G.A., Le, L., Wagstaff, J., and Crozaz, G. (1994) Experimental partitioning of rare earth elements and strontium: Constraints on petrogenesis and redox conditions during crystallization of Antarctic angrite Lewis Cliff 86010. Geochimica et Cosmochimica Acta, 58, 2911–2919.

Moffatt, W.G. (1986) The handbook of binary phase diagrams. Genium Publishing Corporation, New York.

Pownceby, M.I. and O'Neill, H.St.C (1994) Thermodynamic data from redox reactions at high temperatures. IV. Calibration of the Re-ReO$_2$ oxygen buffer from EMF and Ni + Ni-Pd redox sensor measurements. Contributions to Mineralogy and Petrology, 118, 130–137.

Skinner, H.B. and Searcy, A.W. (1973) Mass spectrometric studies of gaseous oxides of rhenium. Journal of Physical Chemistry, 77 , 1578–1585

Stern, C.R. and Wyllie, P.J. (1975) Effect of Fe absorption by noble-metal capsules on phase boundaries in rock-melting experiments at 30 kilobars. American Mineralogist, 60, 681–689.

Weber, B. and Cassuto, A. (1971) Adsorption, désorption et atomisation de l'oxygène sur rhénium. Journal of Chemical Physics, 68, 29–33.

Weber, B., Fusy, J., and Cassuto A. (1970) Mass spectrometric study of the oxygen-rhenium system. In K. Ogata and T.Hayakawa, Eds., Recent Development in Mass Spectrometry, p. 1319–1324. University of Tokyo Press.

Weinbruch, S., Buettner, H., Holzheid, A., Rosenhauer, M., and Hewins, R.H. (1998) On the lower limit of chondrule cooling rates: the significance of Fe loss in dynamic crystallization experiments. Meteoritics and Planetary Sciences, 33, 65–74.

Wimber, R.T. and Kraus, H.G. (1974) Oxidation of iridium. Metallurgical Transactions, 5, 1565–1572.

APPENDIX

The speciation of volatile Re oxides

First of all, we should mention that our experiments on Re metal stability *were not* designed to obtain thermodynamic data. Nevertheless, these are the first systematic data on the effect of f_{O_2} on Re volatility, and our results may possibly be an additional source of thermodynamic information. As noted before, Figure 1 shows the rate of Re volatility as a function of f_{O2} at constant temperature, with three different regions of distinct Re volatility. Volatility in region I is too slow, and in region III is too fast to be treated thermodynamically. We will only try to interpret Re volatility dependence at intermediate f_{O_2} (region II), using a simple thermodynamic model.

Let us assume that, even under our obviously nonequilibrium conditions, loss of Re wire per unit time is proportional to the Re surface area S, to the "equilibrium" partial pressure of volatile Re species p_{vol}, and to the number of Re atoms in the volatile oxide molecule n:

$$-dM/dt = k_1 \times S \times n \times p_{vol} \qquad (A1)$$

where k_1 is a rate constant that is dependent on temperature, gas velocity, etc. Even though gas flow through the furnace precludes the attainment of equilibrium, we assume in the model that the vapor pressure of the primary volatile Re species approaches that of the equilibrium vapor pressure in the vicinity of the Re wire. At least one reason for making this assumption is that, regardless of the rate of gas flow, there will always be a stagnant boundary layer immediately adjacent to the wire surface (Feynman et al. 1964). It is within this small but finite boundary layer that we believe the equilibrium partial pressure is approximated.

Furthermore, if we neglect the ends of the Re wire and assume its length L is constant during the experiment (measurements showed that this assumption is warranted within error limits), the surface area of the wire may be expressed as a function of the mass:

$$S = 2(\pi L/\rho)^{1/2} \times M^{1/2} \qquad (A2)$$

where ρ is the density of Re metal. Combining Equations A1 and A2 yields:

$$-1/M^{1/2} \times dM = 2(\pi L/\rho)^{1/2} \times k_1 \times n \times p_{vol} \times dt \qquad (A3)$$

which can be integrated to give:

$$(M_0^{1/2} - M^{1/2})/t = 2(\pi L/\rho)^{1/2} \times k_1 \times n \times p_{vol} \qquad (A4)$$

where M_0 and M are, respectively, the masses of the Re wire before and after processing in the furnace for a time t. Expressing L through M_0 and the initial radius of the wire R_0, the final equation will be given as:

$$[1 - (M/M_0)^{1/2}]/t = 2k_1 \times n \times p_{vol}/(R_0 \times \rho). \qquad (A5)$$

Alternatively, we can modify Equation A4 and express M and M_0 through the initial and final radii of wire:

$$(R_0 - R)/t = (2k_1 \times n \times p_{vol})/\rho \qquad (A6)$$

Let us designate the left-hand sides of Equations A5 and A6 as $\varphi(M)$ and $\varphi(R)$, respectively, and see how they should depend on f_{O_2}. The general case of the reaction of Re with oxygen to produce volatile species can be written as:

$$n \text{ Re (metal)} + m/2 \text{ O}_2 = \text{Re}_n\text{O}_m \text{ (volatile species)} \qquad (A7)$$

with the constant of equilibrium K_{A7} to be equal:

$$K_{A7} = p_{vol}/(f_{O_2})^{m/2} \times (a_{Re})^n \qquad (A8)$$

For pure Re metal $a_{Re} = 1$; and combining Equation A8 with A5 or A6, after simplification yields:

$$\log\varphi(M) = m/2 \times \log f_{O_2} + \text{CONST} \qquad (A9)$$

or:

$$\log\varphi(R) = m/2 \times \log f_{O_2} + \text{CONST} \qquad (A10)$$

Thus, the slope of $\log\varphi(M)$ or $\log\varphi(R)$ vs. $\log f_{O_2}$ will reflect the number of oxygen atoms in the volatile Re species. For example, in the case of Re_2O_7, the slope should be equal 7/2.

On Appendix Figure 1, we plot $\varphi(M)$ vs. $\log f_{O_2}$. In principle, because we normalize to the length L, two different pieces, exposed to the same conditions, should have the same $\varphi(M)$. This is not exactly the case; smaller lengths of Re wire have slightly lower values of $\varphi(M)$. This is possibly due to our experimental design: longer wires touched the containing crucible only at two end points, whereas short ones lay on the bottom, perhaps slightly decreasing the surface area. Also shown on Appendix Figure 1 and a series of lines with slopes of 1/2 (ReO), 1 (ReO_2), 3/2 (ReO_3), and 7/2 (Re_2O_7) that would be expected for the corresponding species. A linear regression of eight experimental points between $10^{-5.8}$ (RE5) and $10^{-8.0}$ atm (RE7 and RE7a) gives a slope of 1.06 ± 0.04 (1σ; $R^2 = 0.99$), with the apparent Re volatile species being ReO_2. This was unexpected because the calculations using present thermodynamic data (Knacke et al. 1991; Barin 1995) indicate that Re_2O_7 should be the main volatile species at such high temperatures. We will discuss this result in more detail below.

Another way to arrive at this result is to measure wire diameter, rather than wire mass. Monitoring wire diameter is a classical technique for the measurement of evaporation rate (see, for example, Wimber and Kraus 1974), but in our experiments Equation A8 is not as accurate as Equation A9 because of the poorer precision of measurement of small changes in wire diameter, but useful as an independent check of our results. Different wires, exposed to the same conditions, showed the same or very similar diameter within error (see Table 1), so for each distinct experimental condition, an average $\varphi(R)$ was calculated. A linear regression of these averages within the Region II f_{O_2} range gives a slope of 1.00 ± 0.10 (1σ) with $R^2 = 0.97$, in excellent agreement with Appendix Figure 1.

As noted above, Re_2O_7 has been widely believed to be the species responsible for Re metal volatility (e.g., Cotton and Wilkinson 1966). However, a careful survey of the literature showed that the situation is not so clear cut. Indeed, at low temperatures and high f_{O_2} values (above pure solid Re_2O_7 or ReO_3, or above a mixture of Re_2O_7/ReO_3, Re/ReO_2, or ReO_2/ReO_3), Re_2O_7 is the dominant volatile species (Battles et al. 1968; Skinner and Searcy 1973). However, a mass-spectrometric study of a mixture of Re with ZnO at temperatures from 1047 to 1267 K indicated that ReO_3 gas is present in concentrations similar to Re_2O_7 gas, and a reaction of Re with MgO at temperatures from 1770 to 2143 K principally produces ReO_3 gas (Skinner and

Searcy 1973). Moreover, in the case of the last reaction, the authors also found ReO_2^+ and ReO^+ ions, with relative intensities lower than the intensity of the ReO_3^+ ion by factors of 3 and 10, respectively. But these minor ions were interpreted to be the result of dissociative ionization of ReO_3 gas.

Lastly, Weber et al. (1970) conducted a mass-spectrometric study of the evaporation of Re ribbons at low f_{O_2} (in an ultra-high vacuum apparatus). They found that at temperatures below 1800 K only ReO_3 vapor was formed, but at higher temperatures, ReO_2 was observed to form. Franklin and Stickney (1971) derived the thermochemical properties of ReO_3 and ReO_2 from the experimental data of Weber et al. (1970) and Weber and Cassuto (1971). Accordng to our extrapolation of these data, the volatile ReO_3 rather than Re_2O_7 should predominate in a vapor above the Re metal at temperatures higher than 1640 °C.
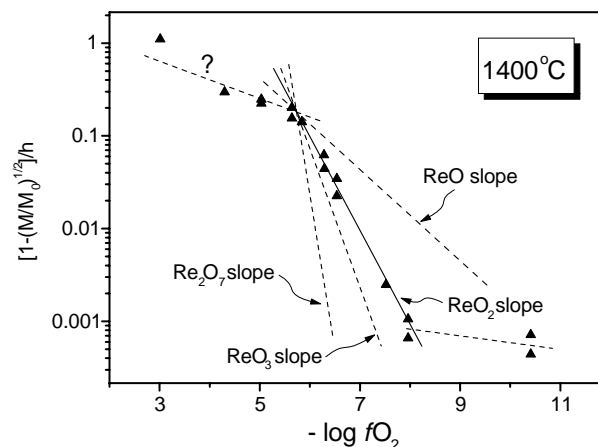
Thus, the issue of Re oxidation may be more complicated than is currently assumed. In particular, in some of the studies cited above, it is not even clear what the source of oxygen is. For example, the extremely large difference between the Mg/MgO and Re/ReO_2 oxygen buffers would seem to preclude MgO as a source of oxygen in the experiments of Skinner and Searcy (1973).

Regardless of the exact stability fields of these Re oxide species, the studies cited above serve to indicate that the thermodynamic basis for solid Re/volatile oxide equilibria is constrained relatively poorly. Even fairly recent data on Re_2O_7 gas from Knacke et al. (1991) were excluded from a later summary (Barin 1995), and more recent electrochemical measurements of Re/ReO_2 equilibrium also require a significant modification to previous estimates on the standard enthalpy of formation of ReO_2 (Pownceby and O'Neil 1994). Furthermore, we wish to emphasize that in our own experiments, we have not directly measured the volatile Re species, and it is possible that the rate of Re volatility is determined by the formation of an intermediate, metastable compound. For example, the volatilization of Re may occur first by the oxidation of Re to ReO_2 (rate limiting step) with subsequent rapid conversion of ReO_2 to Re_2O_7. In our view more work is needed to unravel the detailed systematics of Re oxidation/volatilization.
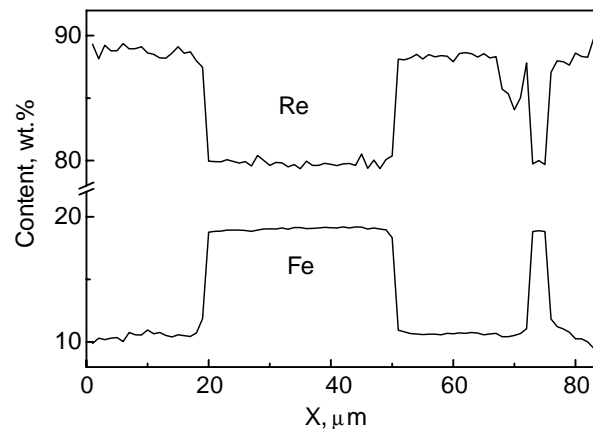
The DAF40-4 loop: Phase relationships in the Re-rich part of the Re-Fe system at 1400 °C

The Re-Fe phase diagram is only known for the Fe-rich side of this binary with Fe ≥ 40 at%, and all additional information about the Re-rich side will be useful. We have already mentioned that the most reducing loop (DAF40-4) was seriously deformed after the experiment. Appendix Figure 2 shows that the Re in this charge apparently reacted to form two coexisting Re-Fe alloys, one having ≈19.0 wt% (44 at%) Fe and the other ≈10.5 wt% (28 at%). We suspect that we may have formed stoichiometric (or nearly stoichiometric) intermetallic compounds such as Re_5Fe_4 (19.4 wt% Fe) and Re_5Fe_2 (10.7 wt% Fe). As

indicated by Appendix Figure 2, Fe and Re concentrations within individual spatial domains are relatively constant, suggestive of stoichiometric phases. In addition, both the absolute Fe concentrations and the lack of Fe concentration gradients in Appendix Figure 2 contrast with those of Figure 4, where simple diffusion appears to be the dominant mechanism for incorporating Fe into Re. Although the Re-rich side of the Re-Fe phase diagram is not known, Re_3Fe_2 and Re_2Fe are believed to be stable in this system (Moffatt 1986), and it is possible that other intermetallics could exist as well.

APPENDIX FIGURE 1. Rate of weight loss of Re wire vs. oxygen fugacity. The parameter $[1-(M/M_0)^{1/2}]/t$ comes from a physical-chemical model for Re volatility (see text for details).

APPENDIX FIGURE 2. An example of an Fe profile through the of DAF40-4 Re loop, the most-reducing and FeO-rich experiment. The loop appears to be a mixture of two stoichiometric Re-Fe intermetallic compounds (see text for details). We were unable to evaluate this possibility further, because the Re rich side of the Re-Fe binary phase diagram has not been well studied.